

## Article

# Particle Deposition Distribution of Multi-Rotor UAV-Based Fertilizer Spreader under Different Height and Speed Parameters

Cancan Song<sup>1,2</sup>, Lilian Liu<sup>1,2</sup>, Guobin Wang<sup>1,2,\*</sup> , Jingang Han<sup>1,2</sup>, Tongsheng Zhang<sup>1,2</sup> and Yubin Lan<sup>1,2,\*</sup>

<sup>1</sup> College of Agricultural Engineering and Food Science, Shandong University of Technology, Zibo 255049, China

<sup>2</sup> Sub-Center of National Center for International Collaboration Research on Precision Agricultural Aviation Pesticide Spraying Technology, Shandong University of Technology, Zibo 255049, China

\* Correspondence: guobinwang@sdut.edu.cn (G.W.); ylan@sdut.edu.cn (Y.L.)

**Abstract:** As an effective supplement to ground machinery, UAVs play an important role in agriculture and have become indispensable intelligent equipment in the development of precision agriculture. Various types of agricultural UAV-based spreading devices, mainly disc-type and pneumatic-type, have appeared in domestic and foreign markets. UAV-based rice topdressing has gradually become a widely recognized application with great market potential. In the process of UAV-based low-altitude fertilization, due to the existence of the rotor wind field, the environment for particle air diffusion is complex, and the movement trajectory and deposition distribution of fertilizer are affected by many factors, resulting in large differences in the spreading. The flight height and speed have a great influence on particle movement and deposition, and a reasonable combination of work parameters can be used for efficient and high-quality particle deposition. In order to obtain better particle deposition distribution, this paper uses the method of a single flight line to test and analyze the characteristics of particle deposition distribution for fertilization using multi-rotor UAVs at different flight heights and speeds. The effective swath width and deposition uniformity obtained via the simulation of overlapped route superposition were used to optimized the appropriate work parameters to ensure that a reasonable and effective deposition amount can be obtained during actual application. The results show that the flight height and speed and the interaction of both have an important influence on the deposition amount and the effective width, but it is not a simple linear relationship. On the whole, as the flight height increases, the coefficient of variation decreases and the effective width increases, but it is not obvious when the speed is low. For the R20, when the flight speed is 2 m/s, the effective width first increases and then decreases with the increase in flight height, and the difference in the deposition amount at a height of 5 m is larger than that at other heights. Under the three working heights, the effective swath width is the same when the flight speed is 4 m/s and 6 m/s, and the effective swath width is also the same when the speed is 7 m and 9 m. For the T16, when the flight speed is 4 m/s, the deposition uniformity is relatively good, and the effective width increases with the increase in flight height. Therefore, the combination of 7–6 m/s and 9–4 m/s parameters will be the best operating parameters for R20 and T16. However, considering the actual dynamic meteorological environment in the field, the operating height can be appropriately lowered according to the influence of the crosswind during actual operation. The research results of this paper can provide scientific reference and suggestions for further improving the effect of UAV-based fertilization.

**Keywords:** agricultural UAV; fertilization; operation parameters; swath width; uniformity



**Citation:** Song, C.; Liu, L.; Wang, G.; Han, J.; Zhang, T.; Lan, Y. Particle Deposition Distribution of Multi-Rotor UAV-Based Fertilizer Spreader under Different Height and Speed Parameters. *Drones* **2023**, *7*, 425. <https://doi.org/10.3390/drones7070425>

Academic Editors: Diego González-Aguilera and Görres Grenzdörffer

Received: 21 March 2023

Revised: 8 June 2023

Accepted: 23 June 2023

Published: 26 June 2023



**Copyright:** © 2023 by the authors. Licensee MDPI, Basel, Switzerland. This article is an open access article distributed under the terms and conditions of the Creative Commons Attribution (CC BY) license (<https://creativecommons.org/licenses/by/4.0/>).

## 1. Introduction

As one of the main food crops in the world, rice has a large demand for chemical fertilizers (nitrogen application amounts of 225.00 kg/ha) [1]. Rational fertilization is the basis and guarantee for obtaining high-quality and high-yield rice, which is of great

significance to food safety [2]. Topdressing outside the root at the late stage is extremely important for the growth of rice. In order to improve fertilizer efficiency under the premise of ensuring sufficient nutrient supply, it is necessary to carry out topdressing several times with a small amount during the critical growth period of rice (such as the tillering stage, heading stage, and booting stage). Nitrogen fertilizer (granule urea) is the main topdressing fertilizer, of which the applied amount accounts for about 45–50% of the whole growth period [3]. However, due to the constraints of small rice planting row spacing, high rice canopy, unclear row ridges, and complex paddy field environments, it is difficult for large-scale ground machinery to enter paddy fields for topdressing operations in the late growth stages, and artificial topdressing is still used in quite a few areas [4]. Artificial topdressing is not only costly and inefficient, but it is also easy to miss the best topdressing node, affecting the growth of rice, resulting in reduced yield and quality.

Agricultural UAVs can fly at low height and high speed to avoid contact with the ground and crops, which is more suitable for the late-stage topdressing application of rice than ground machinery [5–7]. After years of research, UAV spreading technology has developed rapidly, different types of spreading devices based on UAVs have appeared, and its application in the field of fertilization has also been more and more recognized [8–11]. UAV spreading technology mainly include disc type and pneumatic type. The disc-type spreading device has a simple structure and mainly includes two parts: a particle flow control mechanism and a centrifugal disc [12]. During operation, the centrifugal force generated by the high-speed rotation of the disc will scatter the particle falling on the disc from the control mechanism, forming a larger width [13]. The disc-type spreading device has high work efficiency, but the particle trajectory is complex and will form a ring-shaped deposition distribution area, which is difficult to control. Several methods were studied to improve the particle deposition effect through increasing the cover of the disc and changing the radian of the disc [14,15]. The pneumatic-type spreading device is mainly composed of a pneumatic diversion channel, which can use high-speed airflow to blow the particles to move along the pneumatic channels at different angles, increasing the control of the particle diffusion area in the air. At present, various types of pneumatic-type spreading devices such as two-channel [16], four-channel [17], five-channel [18], and collection-row types [19] have been developed. In addition, several UAV companies have launched commercial UAV spreading products [20,21]. Because of continuous technical iteration and structural optimization, UAV spreading technology has been improved, and the application and demonstration area has gradually expanded, which can provide a reliable work platform for field fertilization [22,23].

The most important thing in the rice topdressing operation is to ensure the amount of fertilizer deposition and operation efficiency. In addition to mature spreading devices and technologies, the setting of operation parameters will also have a greater impact on the UAV fertilization [24,25]. Compared with ground fertilization machinery, UAVs rely on rotor lift for low-altitude operations, and particles move in the rotor wind field for a long time. Changes in the operating parameters of the UAV will cause changes in the rotor wind field, thereby affecting the particle deposition distribution state [26,27]. The flight height determines the movement time of the particle in the air after leaving the spreading device. The distribution of the rotor wind field at different heights is quite different, which affects the particle movement trajectory and deposition position [28]. During study of the disc-type UAV spreading device, Chojnacki et al. analyzed the influence of the presence or absence of rotor airflow on the distribution of particle deposition at two operating heights of 0.5 m and 1 m. The results show that the rotor airflow at both heights can accelerate the deposition of particles, resulting in a symmetrical distribution of particles on both sides of the spreading device. Moreover, in the presence of rotor airflow, the difference in the lateral deposition of particles at 1 m is smaller, and the uniformity coefficient of variation is lower than that at 0.5 m, indicating that the rotor airflow at a certain height can improve the effect of particle deposition distribution [29]. The flight speed not only affects the rotor wind field, but also has a certain functional relationship with the particle

discharge amount and fertilizer application rate [30]. Previous studies have pointed out that operation speed and height have a great influence on UAV fertilization effect, but the effects of both on particle deposition distribution have not been thoroughly analyzed. Only through fully understanding the rule of particle deposition under different flight parameters can the operation parameters be reasonably matched and better UAV fertilization effects be obtained.

However, there are few studies on the effect of the height and speed of UAV fertilization on the distribution of particle deposition. In order to obtain effective and uniform fertilizer particle deposition, this paper intends to study the influence of flight parameters on the particle deposition effect for typical disc-type and pneumatic-type UAV spreading devices. Through analyzing particle deposition distribution patterns, effective swath width, and uniformity at different flight speeds and heights, reasonable flight parameters and suggestions for different UAV spreading devices can be given, providing a basis of decision-making for in-field fertilization.

## 2. Materials and Methods

### 2.1. Test Devices and Materials

The devices and materials used in this test mainly include disc-type and pneumatic-type UAV-based spreading devices, granular fertilizer (medium granular, humic acid urea, nitrogen content  $\geq 46.0\%$ , Henan Xinlianxin Chemical Industry Group Co., Ltd., Xinxiang, China), a particle collector (plastic box, size:  $0.6 \times 0.4 \times 0.28$  m), a sample bag, and an electronic balance (graduation value: 0.1 mg, model: FA2204, brand: Lichen Technology). As shown in Figure 1, the R20 is a pneumatic-type spreading device based on a six-rotor UAV. The R20 has 5 pneumatic diversion channels, and the average air velocity at the outlet of the diversion channels can reach more than 9.5 m/s. The T16 is a disc-type spreading device based on a six-rotor UAV (Shenzhen DJI Co., Ltd., Shenzhen, China), with a disc diameter of 24 cm. Both spreading devices of the two types of fertilization UAV were installed directly below the body of the UAV, where the rotor flow is weak. During operation, the fertilizer output status of the two kinds of spreading devices is different. The fertilizer outlet of the pneumatic spreading device is behind the fuselage and parallel to the airline line, and the particles are gradually dispersed in the air, while the particles of the disc spreading device are dispersed around the disc to form a ring dispersion area. The detailed parameters of the two tested devices are shown in Table 1.



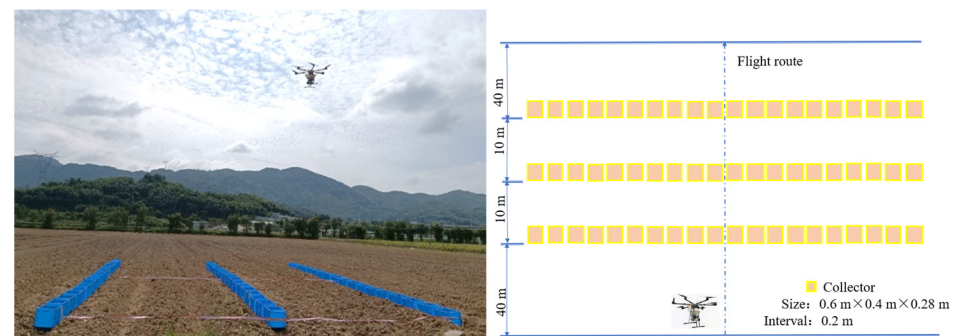
**Figure 1.** The UAV spreading devices for test. (a) R20, (b) T16.

**Table 1.** The main parameters of the tested UAV spreading devices.

Parameters	R20	T16
Manufacturer	self-developed	DJI
Model	R20	T16
Rotor	6	6
Power supply	electric	electric
Max work voltage (V)	50	58.8
Effective load (kg)	20	16
Flight height (m)	$\leq 30$	$\leq 30$
Flight speed (m/s)	$\leq 7$	$\leq 10$
Spreading type	pneumatic-type	disc-type
Particle size (mm)	0.5~5	0.5~5
Discharge range (kg/min)	22	60

## 2.2. Experiment Design

According to the standards of American Society of Agricultural and Biological Engineers (ASABE S341.5) [31], the method of deposition distribution testing in a single route was adopted in this paper. The test area is divided into an acceleration area, a constant speed area, and a deceleration area. In the constant speed area, three particle sampling belts are set up along the route direction, with an interval of 10 m. The total length of the sampling belt is 12.4 m, and 18 collectors are set in each belt with an interval of 0.2 m between adjacent collectors to ensure that the particle deposition range under all test conditions can be covered. During the flight along the route, the UAV spreads fertilizer particles while passing through the particle collection area. Fertilizer particles at all sampling points were collected and weighed to obtain the deposition amount of per unit area. Through setting different flight heights and speeds, the particle deposition distribution under different conditions can be obtained. The specific test plan and sampling point layout are shown in Figure 2.

**Figure 2.** Test site and sampling point layout.

According to the operation experience of agricultural UAV, the flight height of fertilization is relatively high. The flight heights of this test are set as 5 m, 7 m, and 9 m, and the flight speeds are 2 m/s, 4 m/s, and 6 m/s. Due to the different spreading principles and discharge control methods of the two tested devices, in order to avoid the interference of other factors and obtain effective test results, the discharge rate in this test was set to 5 kg/min. According to pre-experiments, the average air velocity in the air channel for R20 is 9.6 m/s, and the rotation speed of the disc for T16 is set to 1000 r/min to ensure the same deposition width under the same operating conditions. During the test, the battery power is not less than 50%, the amount of fertilizer in the hopper is not less than 60% of the capacity, and the rest of the parameters are set according to the actual operation requirements. The test was repeated twice under each operating parameter, and the meteorological data, flight time, and actual spreading amount were recorded during all tests. The specific experimental design of factor parameters is shown in Table 2.

**Table 2.** The experimental design of factor parameters.

Treatment	Flight Height (m)	Flight Speed (m/s)
T1	5	2
T2	5	4
T3	5	6
T4	7	2
T5	7	4
T6	7	6
T7	9	2
T8	9	4
T9	9	6

### 2.3. Analytical Indicators and Calculation Methods

#### 2.3.1. Deposition Amount

Deposition amount refers to the deposition amount per unit area calculated according to the fertilizer amount in the collector after each route is executed. The calculation formula is as follows:

$$Q = M/S \quad (1)$$

where  $Q$  is the actual deposition amount,  $g/m^2$ ;  $M$  is particle quantity in the collector,  $g$ ;  $S$  is the bottom area of the collector, and the constant value is  $0.24 m^2$ .

In this paper, three deposition curves will be obtained under each test, and the difference should be determined through variance analysis. At each treatment, the average value of six deposition amount values at each sampling point under 2 repetitions will be used as the actual deposition volume under this treatment.

#### 2.3.2. Effective Swath Width and Uniformity

The particle deposition swath width is calculated via the simulation of routes overlapped method. As shown in Figure 3, the deposition distribution curve measured under a single route is overlapped according to the reciprocating method of the UAV executing multiple routes (3–5 deposition curves are overlapped), The overlapped increment is an integer multiple of the interval between two collectors. The uniformity variation coefficient (CV) of the new deposition curve after each overlap is calculated according to Formula (2), and the overlapped increment associated with the minimum acceptable CV (The widest used in fertilizer is  $CV < 20\%$ .) shall be considered the effective swath width of the test. The specific formula is as follows:

$$\bar{M} = \frac{\sum M_i}{n}, SD = \frac{\sqrt{\sum_1^n (M_i - \bar{M})^2}}{n - 1}, CV = \frac{SD}{\bar{M}} \times 100\% \quad (2)$$

where  $M$  is the deposition amount between the centerlines of the first and third deposition curves after the deposition curves are overlapped,  $g/m^2$ ;  $\bar{M}$  is the mean value,  $g/m^2$ ;  $n$  is the sampling number of overlapped deposition curves.

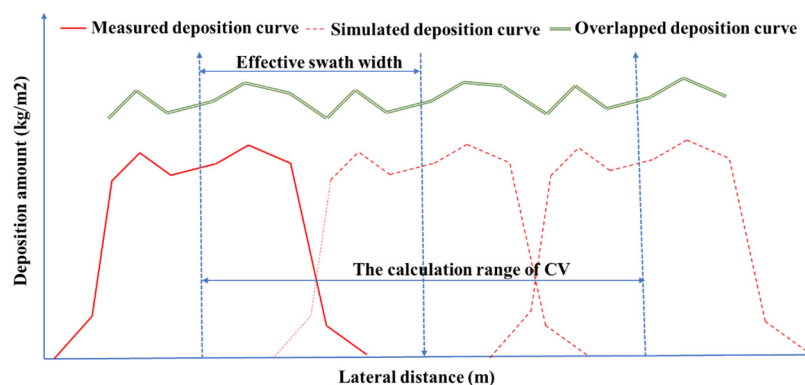


**Figure 3.** Graphical presentation of effective swath width and CV.

### 3. Results and Analysis

#### 3.1. Distribution of Deposition Amount under Different Operating Parameters

Figures 4 and 5 show the deposition curves of the average value of the six particle deposition distribution curves under each treatment. The results of variance analysis showed that there was no significant difference in the deposition amount data of the six groups of deposition amount under two repetitions ( $p$ -value > 0.05). On the whole, the particle deposition distribution curves obtained for the two tested devices are mostly normally distributed, and the deposition amount gradually decreases from the center of the route to both sides. The results of variance analysis under different work conditions showed that the flight height and speed and the interaction between them had a very significant effect on the amount of fertilizer deposition ( $p$  value = 0.00). As shown in Figure 4, for R20, the decline in deposition amount is relatively large, and the curve fluctuates greatly. Especially when the flight speed is low (2 m/s), the waist of the triangle is steep, and most particles gather near the center of the flight path. When the flight speed is high (especially 6 m/s), the shape of the deposition curve changes from a triangle to a trapezoid, and the horizontal straight line near the center of the course lengthens and tends to be stable.

As shown in Figure 5, for T16, the deposition curve changes smoothly, and as the speed increases, the slope of the triangle gradually decreases. The range of particle deposition amount of the two tested devices is basically the same (the maximum of R20 is about 6 g/m<sup>2</sup>, and the maximum amount of T16 is about 5.5 g/m<sup>2</sup>). With the increase in flight speed, the deposition amount also decreases, which is consistent with the actual situation. In addition, when the flight speed and height are large, the deposition amount in a certain range (−2.8 m~2.8 m) near the center of the flight route of R20 tends to be stable, while the particle deposition amount of T16 keeps decreasing from the center of the flight route to the two edges, causing a smaller difference than that of R20. In addition, the deposition amount of both spreader devices is influenced by lower flight speed at all flight heights. When the flight speed increases from 2 m/s to 4 m/s, the maximum deposition amount decreases by about half, while the difference decreases when the flight speed increases from 4 m/s to m/s 6. That is to say, at a low flight speed, the influence of flight speed is greater than that of height, and as the speed increases, the effect of height on deposition amount gradually increase.

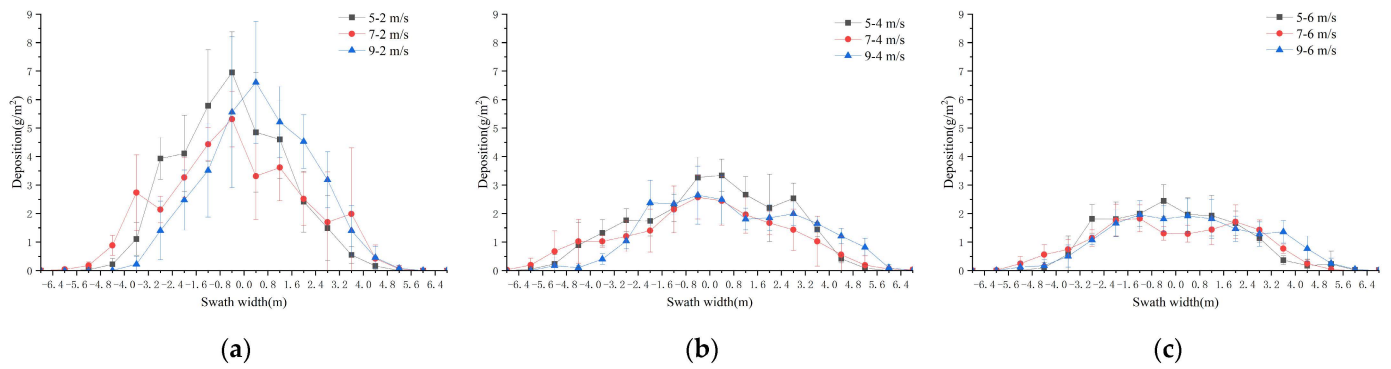


**Figure 4.** The particle deposition distribution of R20. (a) Flight speed is 2 m/s. (b) Flight speed is 4 m/s. (c) Flight speed is 6 m/s.

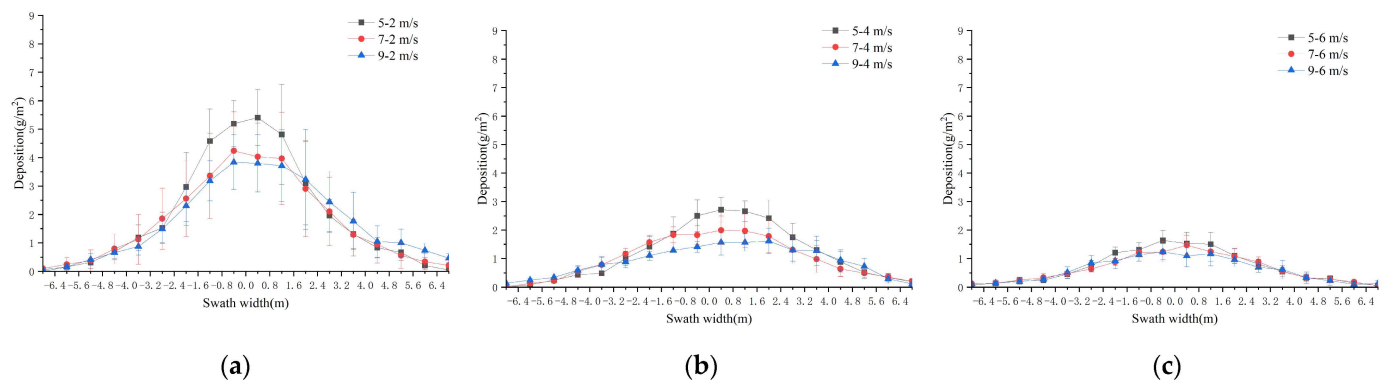


**Figure 5.** The particle deposition distribution of T16. (a) Flight speed is 2 m/s. (b) Flight speed is 4 m/s. (c) Flight speed is 6 m/s.

3.2. Analysis of Effective Width and Uniformity

The relationship between the CV and overlapping increment of the deposition curve obtained via the simulation of routes overlapped method is shown in Figures 6 and 7. In Figure 6, with the continuous increase in the overlapping increment, the CV value fluctuates to varying degrees within a certain range, but then it shows a gradually increasing trend. In Figure 7, the CV value gradually increases with the increase in the overlapping increment, but the magnitude of the increase is different. This is mainly because the shapes of the particle deposition distribution curves formed by the two spreading devices are different, and the deposition amount after overlapping changes in different laws.

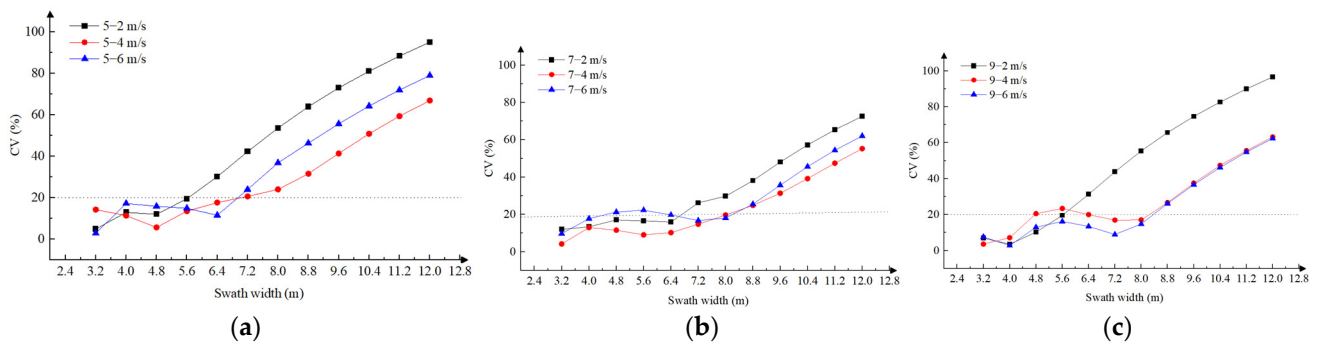


**Figure 6.** Swath width and CV of overlapped deposition distribution data for R20. (a) Flight height is 5 m. (b) Flight height is 7 m. (c) Flight height is 9 m.

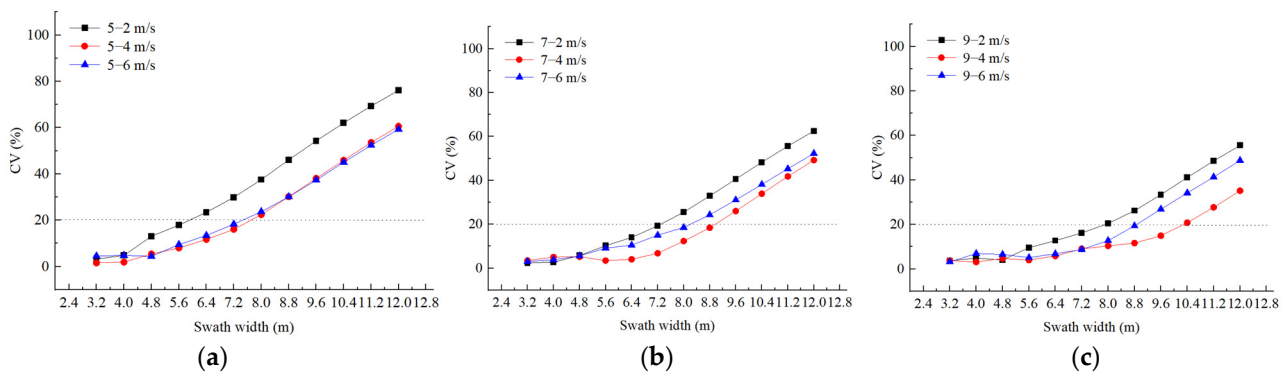


**Figure 7.** Swath width and CV of overlapped deposition distribution data for T16. (a) Flight height is 5 m. (b) Flight height is 7 m. (c) Flight height is 9 m.

For R20, due to the large fluctuation of the deposition curve, with the increase in the overlap increment, the deposition amount of the overlapping part will exceed or approach the maximum deposition amount in the center line of the deposition curve, resulting in a large CV of the overall deposition amount. fluctuation. However, as the overlapping part of the depositional curves decreases, the difference between the overlapped deposition amount and the maximum deposition amount on the centerline of the depositional curves gradually increases, so the CV value also increases significantly. It can also be seen from Figure 5 that in the section of CV value fluctuation, the fluctuation range is the largest when the flight speed is 6 m/s, and in the section where CV value gradually increases, the CV value first exceeds the standard line ( $CV = 20\%$ ) when the flight speed is 2 m/s; it reaches the maximum when the flight height is 9 m, which is significantly different from other flight speeds. In addition, the CV values at the flight height of 7 m and 9 m exceeded the standard line in the section of CV value fluctuates (7–6 m/s and 9–4 m/s, respectively), but did not exceed at the flight height of 5 m, which shows that when the working height and speed are high, the particle deposition distribution is easily affected, resulting in a larger and more unstable deposition distribution area.

For T16, since the shape of the triangular depositional curve is relatively smooth, the deposition amount decreases sequentially. The difference between the deposition amount in the overlapping part of the deposition curve and the deposition amount in the center line of the deposition curve is small, and the overall uniformity is good. Therefore, the CV value gradually increases without large fluctuation, as the increase in the overlap increment. It can also be seen from Figure 6 that, compared with other flight speeds, the CV value first exceeds the standard line when the flight speed is 2 m/s. At the same height, with the increase in flight speed, the intersection point of the CV value and standard line gradually moves back, and the same change happens as the flight height increases at the same flight speed. These changes show that the effective deposition distribution area and deposition amount of the overlapped deposition curves obtained at higher flight speeds and heights increase, which means the route spacing could be larger under the premise of ensuring that the uniformity meets the requirements of the fertilization target.

The effective swath width and CV obtained via the simulation of routes overlapped method under different work parameters are shown in Table 3. The maximum overlap increment when the CV gradually approaches the standard line ( $CV = 20\%$ ) is the effective swath width. The deposition amount is the mean of the amount overlapped by multiple deposition curves. The deposition amount decreases with the increase in the flight speed and has no obvious relationship with the working height for both tested UAVs. However, except for the large difference in deposition amount under the parameter of 5–2 m/s, the reduction ranges under the other work parameters are basically the same for R20. The reason of this difference may be that R20 uses a multi-channel pneumatic method to blow particles, and the wind speed at the outlet closest to the wind source is relatively higher, resulting in a slightly larger particle flow in this channel, which eventually forms a

relatively large deposition amount near the flight route. For T16, the annular deposition distribution shape will cause the accumulation of deposition near the central flight route, which is determined via the centrifugal disc mechanism.

**Table 3.** The effective swath width and uniformity of tested UAVs in different work parameters.

Treatment	Flight Height (m)	Flight Speed (m/s)	R20			T16		
			Mean of Deposition Amount (g/m <sup>2</sup> )	Effective Swath Width (m)	CV (%)	Mean of Deposition Amount (g/m <sup>2</sup> )	Effective Swath Width (m)	CV (%)
T1	5	2	8.24	5.6	19.49	5.05	5.6	17.88
T2	5	4	3.04	6.4	17.65	2.33	7.2	16.07
T3	5	6	2.03	6.4	11.53	1.38	7.2	18.33
T4	7	2	4.03	6.4	15.93	3.48	7.2	19.28
T5	7	4	1.99	8.0	19.70	1.64	8.8	18.41
T6	7	6	1.44	8.0	18.09	1.15	8.0	18.53
T7	9	2	5.06	5.6	19.58	3.49	7.2	16.21
T8	9	4	2.12	8.0	17.02	1.36	9.6	14.94
T9	9	6	1.63	8.0	14.77	0.98	8.8	19.39

The data in Table 3 show that for both tested UAVs, the overall effective swath width increases with increasing flight height and flight speed. When the flight height and speed increase, the average effective width of R20 increases from 5.6 m to 8.0 m, and the average effective swath width of T16 increases from 5.6 m to 9.6 m. However, the relationship between the effective swath width and flight speed and height is not simply linear. For R20, under the three working heights, the effective swath width is the same when the flight speed is 4 m/s and 6 m/s, and the effective swath width is also the same when the speed is 7 m and 9 m. For T16, the effective swath width is the same when the work parameters are 5–4 m/s, 5–6 m/s, 7–2 m/s, and 9–2 m/s. When the flight height is 7 m and 9 m, the effective swath width first increases and then decreases with the increase in the flight speed, and the fluctuation range becomes larger. The above results indicate that the interaction between flight height and speed will affect the particle deposition width. In terms of uniformity, the CVs of R20 and T16 are all lower than 20%, which is acceptable for field application.

### 3.3. Analysis of Deposition Amount Simulation

The deposition curve drawn according to the deposition amount after the simulation of overlapped routes is shown in Figure 8. It can be seen that from the center to both sides of the deposition curve, the deposition amount fluctuates up and down in a straight line. The deposition curve is obtained through overlapping the multiple deposition curves from a single route, which is essentially formed through the translation and replication of a deposition curve, so the fluctuation is regular. In addition, the overlapped deposition curves of the tested UAVs are affected by work parameters to varying degrees. When the flight speed is low, the deposition amount fluctuates greatly, and the overall lateral uniformity is poor, but when the flight speed and height increase, the deposition curve tends to be flat and stable. The overlapped deposition curve shown in Figure 7 is obtained through simulating the overlapped flight routes of UAV, the change of which can reflect the actual deposition distribution characteristics to a certain extent. This figure shows that uniform fertilizer deposition distribution and high efficiency could be realized when the flight height and speed are in the appropriate range (for example, 5–6 m/s, 7–4 m/s, 7–6 m/s, 9–4 m/s, and 9–6 m/s). Therefore, it is necessary to select a reasonable combination of flight parameters according to the characteristics of different models in field application, rather than determining the best height and speed.

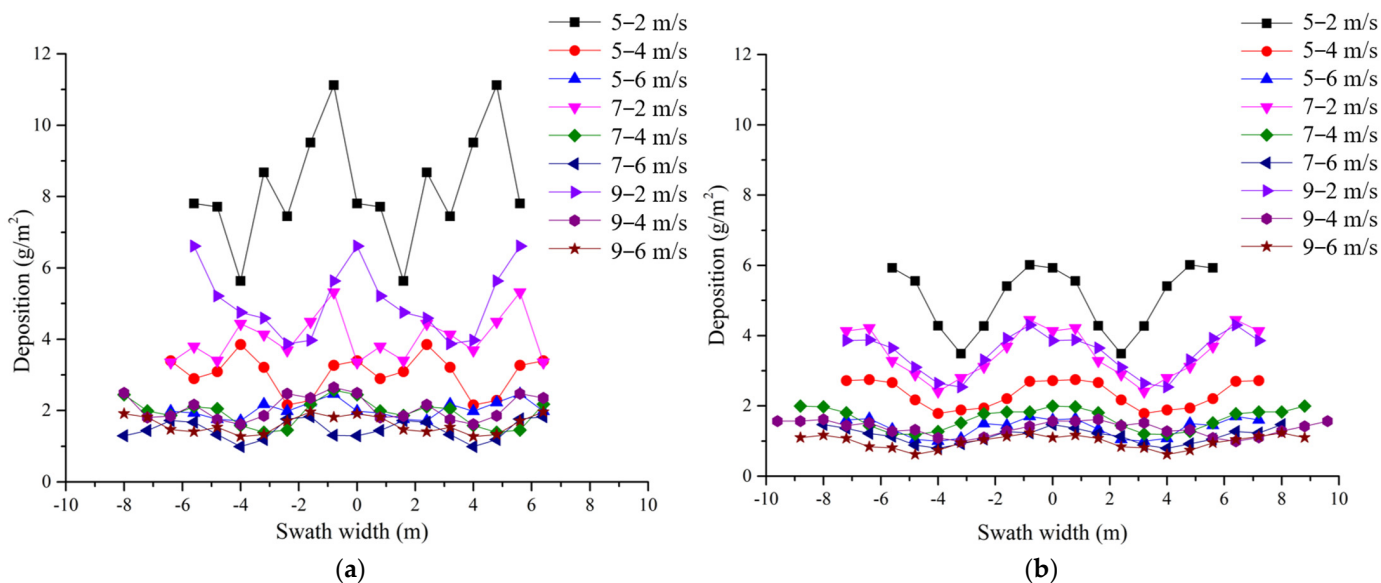


Figure 8. The overlapped deposition cures of two tested UAVs. (a) R20, (b) T16.

#### 4. Discussion

The statistical method of fertilizer particles used in this paper is to collect samples from the field and then take them back to the laboratory for weighing, rather than real-time detection. Compared with the particle identification method using image detection technology, the efficiency is lower. In addition, in recent related research, computer simulation technology is increasingly used to simulate the trajectory of granular particles. Although this method is low in cost and short in time, it cannot completely simulate the field environment to obtain the real deposition data of in-field UAV fertilization. Compared with more mature computer simulations, the field test is more affected by environmental factors, but it can reflect the actual particle deposition distribution, which is of great value and significance for the optimization of operation parameters and prediction of particle deposition distribution in the later period.

In the low-altitude fertilization of agricultural UAVs, due to the existence of the rotor wind field, the work parameters have a great influence on the particle deposition distribution. Theoretically, the amount of deposition decreases gradually with the increase in velocity, and the width of lateral deposition increases with the increase in height. The research results of this paper showed that the effective width and uniformity will not always get better with the increase in flight height and speed. When the speed increases from 2 m/s to 4 m/s, the deposition amount is halved, but when the speed is from 4 m/s to 6 m/s, the deposition amount is not halved, and the swath width increases accordingly, indicating that the particle diffusion movement is affected by the flight speed. With the increase in flight altitude, the increase in depositional width is smaller. For example, for R20, there is a lower effective width (5.6 m) at the height of 9 m and 5 m, and there is also a higher effective width (8.0 m) at the flight height of 7 m and 9 m. For T16, the effective width of 7.2 m can be achieved at the flight heights of 5 m, 7 m, and 9 m, which shows that the flight speed interferes with the particle deposition results. In addition, the disorderly spreading pattern of the two tested UAVs makes it difficult to achieve high uniformity in the particle deposition on the ground. For these two spreading devices with different working principles, there are differences in particle motion states, which will inevitably lead to differences in deposition distribution under different operating conditions. For crop growth, the standard line of uniformity coefficient of variation ( $CV = 20\%$ ) used in this paper is sufficient for the field application. Therefore, the appropriate range of work parameters can be selected for different fertilization requirements and machine types.

In addition to the flight height and speed, many other factors affect particle deposition distribution. The research in this paper is carried out under the condition that the particle discharge rate and the UAV platform of the tested spreading devices are basically the same. However, the results of particle deposition will still be disturbed by factors such as the structure of the spreading device and the wind field of the rotor, and even the size and layout of the collector will affect the bouncing of particles and deposition. In addition, the state of the agricultural UAV changes all the time during the flight, and the particle deposition distribution on adjacent routes is inconsistent. Therefore, the deposition amount in the overlapped area is not obtained through a simple overlap of multiple deposition curves. Although the deposition curve obtained via the simulation of overlapped routes is not the actual deposition result, it conforms to the work mode of the UAV. This method is suitable for deposition distribution curves with different shapes and can provide test methods and references for UAV-based spreading devices with different principles.

Agricultural UAV fertilization is a dynamic operating system. The authors studied the effect of two important factors, flight height and speed, on the distribution of particle deposition, which is meaningful, but not enough. The authors used urea granules for their tests and set a fixed air velocity and disc rotation speed for pneumatic and disc spreaders. The deposition distribution results obtained in the test may not be applicable to other material particles or operation requirements. Also, the optimal combination of work parameters obtained from previous tests may not be able to obtain the expected deposition in actual application, and more in-field applications are required. The research results of this paper show that the same effective swath width can be obtained through choosing a flight height of 5 m or 9 m with acceptable uniformity, and a flight speed of 4 m/s or 6 m/s has little effect on particle deposition. Considering the environment and fertilization rate, a lower height and a higher speed can be selected in normal operation, but the operating height can be higher when there is interference from field-side wires and tree crowns, which can reduce energy consumption and improve efficiency. In addition, fertilizer need to be added and batteries need to be replaced frequently in the process of UAV fertilization, which requires more reasonable route planning and parameter setting to ensure that the route break point is close to the fertilization point, avoid wasting more time, and improve work efficiency while ensuring the fertilization deposition effect.

## 5. Conclusions

In this paper, disc-type and pneumatic-type spreading devices based on UAVs are tested under different flight heights and speeds through a single-route deposition distribution test. A simulation of overlapped routes is used to obtain the particle deposition distribution characteristics and the effective swath width and uniformity. According to the influence of flight height and speed on the effect of particle deposition width and uniformity, suggestions were proposed to optimize the parameters of UAV-based fertilization. The specific conclusions are as follows:

- (1) The flight height and speed and their interaction have a very significant effect on particle deposition uniformity and width, but it is not a simple linear relationship. On the whole, as the flight height and speed increase, the effective swath width increases, but due to their interaction, the same swath width could be obtained at different flight heights and speeds. For R20, when the flight height is 7 m and 9 m, a larger effective width ( $CV = 18.09\%$ ) can be obtained at a higher flight speed. For T16, when the flight height is higher, the effective width increases with the working speed first and then decreases. The deposition uniformity does not change much with the influence of flight height and speed, and the corresponding effective width can be used as the maximum route spacing under this condition.
- (2) According to the analysis of deposition results based on the test conditions given in this paper, the combination of 7–6 m/s and 9–4 m/s can not only meet the uniformity requirements, but also improve the working efficiency, which will be the optimal flight parameters for R20 and T16. However, considering the actual dynamic meteorological

environment in the field, the operating height can be appropriately lowered according to the influence of the crosswind during actual in-field operation.

- (3) Since there are many factors affecting UAV-based fertilization, this paper currently only tests the flight height and speed in a limited range. With the improvement of the load and performance of the agricultural UAV, the range of flight height and speed can be expanded in the future, and more suitable parameter ranges can be obtained through continuous tests. At the same time, it is also necessary to study the influence of other factors on the particle deposition distribution and the parameter optimization of the whole spread system.

**Author Contributions:** Methodology, C.S.; investigation, L.L.; resources, G.W.; data curation, T.Z. and J.H.; writing—original draft preparation, L.L.; visualization, Y.L. All authors have read and agreed to the published version of the manuscript.

**Funding:** This work was financially supported by the Shandong Natural Science Foundation Project (ZR2021QC154), Top Talents Program for One Case One Discussion of Shandong Province.

**Institutional Review Board Statement:** Not applicable.

**Informed Consent Statement:** Not applicable.

**Data Availability Statement:** Not applicable.

**Acknowledgments:** The authors are very grateful to the editors and anonymous reviewers for their critical comments and suggestions to improve the manuscript.

**Conflicts of Interest:** The authors declare no conflict of interest.

## References

- Huang, J.; Wu, J.; Chen, H.; Zhang, Z.-X.; Fang, C.-X.; Shao, C.-H. Optimal management of nitrogen fertilizer in the main rice crop and its carrying-over effect on ratoon rice under mechanized cultivation in southeast China. *J. Integr. Agric.* **2022**, *21*, 351–364.
- Zhang, H.; Hou, D.P.; Peng, X.L.; Ma, B.J.; Shao, S.M.; Jing, W.J.; Yang, J.C. Optimizing integrative cultivation management improves grain quality while increasing yield and nitrogen use efficiency in rice. *J. Integr. Agric.* **2019**, *18*, 2716–2731. [[CrossRef](#)]
- Zhang, J.W.; Wang, J.D.; Zhou, Y.; Xu, L.; Chen, Y.L.; Ding, Y.F. Reduced basal and increased topdressing fertilizer rate combined with straw incorporation improves rice yield stability and soil organic carbon sequestration in a rice-wheat system. *Front. Plant Sci.* **2022**, *13*, 964957. [[CrossRef](#)]
- Song, C.C.; Zhou, Z.Y.; Luo, X.W. Review of agricultural materials broadcasting application on unmanned helicopter. *J. Agric. Mech. Res.* **2018**, *40*, 1–9. (In Chinese)
- Zhu, S.L.; Zhou, W.; Zhu, L.; Sun, B.T.; Huang, S.; Wu, Z.Y.; Ren, W. Unmanned air vehicle adaptability and application evaluation for new rice panicle fertilizers: Fertilizer characteristics and mechanical adaptability. *Technol. Agron.* **2022**, *2*, 1. [[CrossRef](#)]
- Aslan, M.F.; Durdu, A.; Sabanci, K.; Ropelewska, E.; Gültekin, S.S. A comprehensive survey of the recent studies with UAV for precision agriculture in open fields and greenhouses. *Appl. Sci.* **2022**, *12*, 1047. [[CrossRef](#)]
- Zhang, C.H.; Kovacs, J.M. The application of small unmanned aerial systems for precision agriculture: A review. *Precis. Agric.* **2012**, *13*, 693–712. [[CrossRef](#)]
- Yang, W.H.; Kim, J.K.; Lee, M.H.; Chen, S.C.; Han, H.S. Status and prospect on rice direct seeding technology of farmers. *J. Korean Soc. Int. Agric.* **2015**, *27*, 342–347. [[CrossRef](#)]
- Yamunathangam, D.; Shanmathi, J.; Caviya, R.; Saranya, G. Payload manipulation for seed sowing unmanned aerial vehicle through interface with pixhawk flight controller. In Proceedings of the Fourth International Conference on Inventive Systems and Control, Coimbatore, India, 8–10 January 2020.
- Marzuki, O.F.; Teo, E.Y.L.; Rafie, A.S.M. The mechanism of drone seeding technology: A review. *Malays. For.* **2021**, *84*, 349–358.
- Liu, W.; Zou, S.; Xu, X.; Gu, Q.; He, W.; Huang, J. Development of UAV-based shot seeding device for rice planting. *Int. J. Agric. Biol. Eng.* **2022**, *15*, 1–7. [[CrossRef](#)]
- Li, J.Y.; Lan, Y.B.; Zhou, Z.Y.; Zeng, S. Design and test of operation parameters for rice air broadcasting by unmanned aerial vehicle. *Int. J. Agric. Biol. Eng.* **2016**, *9*, 24.
- Song, C.C.; Zhou, Z.Y.; Luo, X.W.; Ming, R.; Li, K.L. Design and test of centrifugal disc type sowing device for unmanned helicopter. *Int. J. Agric. Biol. Eng.* **2018**, *11*, 55–61. [[CrossRef](#)]
- Coetzee, C.J.; Lombard, S.G. Discrete element method modelling of a centrifugal fertilizer. *Biosyst. Eng.* **2011**, *109*, 308–325. [[CrossRef](#)]
- Wu, Z.J.; Li, M.L.; Lei, X.L.; Wu, Z.; Jiang, C.; Zhou, L. Simulation and parameter optimisation of a centrifugal rice seeding spreader for a UAV. *Biosyst. Eng.* **2020**, *192*, 275–293. [[CrossRef](#)]

16. Zhu, J.L. A New Solid Material Flow Controllable Spraying Device Based on Unmanned Aerial Vehicle. CN Patent 213215033 U, 18 May 2021. (In Chinese).
17. Li, S.H.; Wen, F. A Spreading Device and Plant Protection Equipment. CN Patent 113508665 A, 19 October 2021. (In Chinese).
18. Song, C.C.; Zhou, Z.Y.; Jiang, R.; Luo, X.; He, X.; Ming, R. Design and parameter optimization of pneumatic rice sowing device for unmanned aerial vehicle. *Trans. Chin. Soc. Agric. Eng.* **2018**, *34*, 80–88. (In Chinese)
19. Huang, X.M.; Zhang, S.; Luo, C.M.; Li, W.; Liao, Y. Design and experimentation of an aerial seeding system for rapeseed based on an air-assisted centralized metering device and a multi-rotor crop protection UAV. *Appl. Sci.* **2020**, *10*, 8854. [[CrossRef](#)]
20. Sowing UAV of DJI [EB/OL]. Available online: <https://ag.dji.com/cn/t50?site=brandsite&from=nav> (accessed on 13 December 2022).
21. Sowing UAV of XGA [EB/OL]. Available online: <https://www.xa.com/p100pro-2023> (accessed on 13 December 2022).
22. Song, C.C.; Zhou, Z.Y.; Zang, Y.; Zhao, L.; Yang, W.; Luo, X. Variable-rate control system for UAV-based granular fertilizer spreader. *Comput. Electron. Agric.* **2021**, *180*, 105832. [[CrossRef](#)]
23. Grafton MC, E.; Irwin, M.E.; Sandoval-Cruz, E.A. Measuring the response of variable bulk solid fertiliser application by computer-controlled delivery from aircraft. *N. Z. J. Agric. Res.* **2022**, *65*, 507–519. [[CrossRef](#)]
24. Hijazi, B.; Cool, S.; Vangeyte, J.; Mertens, K.; Cointault, F.; Paindavoine, M.; Pieters, J.G. High Speed Stereovision Setup for Position and Motion Estimation of Fertilizer Particles Leaving a Centrifugal Spreader. *Sensors* **2014**, *14*, 21466–21482. [[CrossRef](#)] [[PubMed](#)]
25. Villette, S.; Piron, E.; Miclet, D. Hybrid centrifugal spreading model to study the fertiliser spatial distribution and its assessment using the transverse coefficient of variation. *Comput. Electron. Agric.* **2017**, *137*, 115–129. [[CrossRef](#)]
26. Guo, Q.W.; Zhu, Y.Z.; Tang, Y.; Hou, C.; He, Y.; Zhuang, J. CFD simulation and experimental verification of the spatial and temporal distributions of the downwash airflow of a quad-rotor agricultural UAV in hover. *Comput. Electron. Agric.* **2020**, *172*, 105343. [[CrossRef](#)]
27. Song, C.C.; Wang, G.B.; Zhao, J.; Wang, J.; Yan, Y.; Wang, M.; Zhou, Z.; Lan, Y. Research progress on the particle deposition and distribution characteristics of granular fertilizer application. *Trans. Chin. Soc. Agric. Eng.* **2022**, *38*, 59–70. (In Chinese)
28. Song, C.C.; Zang, Y.; Zhou, Z.Y.; Luo, X.; Zhao, L. Test and Comprehensive Evaluation for the Performance of UAV-Based Fertilizer Spreaders. *IEEE Access* **2020**, *8*, 202153–202163. [[CrossRef](#)]
29. Chojnacki, J.; Berner, B. The influence of air stream generated by drone rotors on transverse distribution pattern of sown seeds. *J. Res. Appl. Agric. Eng.* **2018**, *63*, 9–12.
30. Zhang, Q.S.; Zhang, K.; Liao, Q.X.; Liao, Y.T.; Wang, L.; Shu, C.X. Design and experiment of rapeseed aerial seeding device used for UAV. *Trans. Chin. Soc. Agric. Eng.* **2020**, *36*, 138–147. (In Chinese)
31. American Society of Agricultural Biological Engineers. ASABE (S341.5). Procedure for Measuring Distribution Uniformity and Calibrating Granular Broadcast Spreaders, Michigan. 2018. Available online: <https://elibrary.asabe.org/abstract.asp?aid=48938> (accessed on 22 March 2022).

**Disclaimer/Publisher’s Note:** The statements, opinions and data contained in all publications are solely those of the individual author(s) and contributor(s) and not of MDPI and/or the editor(s). MDPI and/or the editor(s) disclaim responsibility for any injury to people or property resulting from any ideas, methods, instructions or products referred to in the content.